JOURNAL OF COMPUTATIONAL PHYSICS 13, 15–34 (1973)

# A Numerical Method for the Solution of Tidal Dynamics Equations and the Results of Its Application

G. I. MARCHUK

*Computer Center of the Siberian Branch of the U.S.S.R. Academy of Sciences, Novosibirsk*

R. G. GORDEEV, V. YA. RIVKIND

*Computer Center of the Leningrad State University, Leningrad*

AND

B. A. KAGAN

*P. P. Shirshov Institute of Oceanology, U.S.S.R. Academy of Sciences, Leningrad*

Received July 19, 1972

For a numerical solution of tidal dynamics equations, the alternating direction scheme is used. The difference scheme is described in detail, and the proof of its stability and convergence is given. The results of application of the method in different geophysical conditions are reported. The calculated charts of isoamplitudes and co-tidal lines as well as those of tidal currents are generally in satisfactory agreement with observational data.

## 1. INTRODUCTION

It is customary to use in tidal calculations numerical methods of integration of tidal dynamics equations. Especially popular are a method of boundary values and a hydrodynamical numerical method (often referred to as HN-method) [1, 2].

The first of the above methods assumes a harmonic nature of variations in time of tidal characteristics. According to this assumption, a system of linearized dynamics equations is reduced to one partial differential equation of elliptic type with respect to complex amplitudes of tidal oscillations of the level. The formulated boundary value problem is solvable, and has a unique solution if the condition $\sigma > l$ (where $\sigma$ is angular velocity of the tidal wave, $l$, the Coriolis parameter) is met, and values of amplitudes are known on the whole contour of a considered basin or on one of its parts, whereas on the other part there is a condition of no





581/13/1-2

transport (this condition is equivalent to formulation of oblique derivative for the level). The solution is found by standard methods, using the first variant of boundary conditions, or by a special numerical method, developed in [3], for Poincare problem, in the case when, on one part of the contour, the boundary condition is in a form of oblique derivative.

If the condition $\sigma > l$ is not met, and a "critical" latitude (on which $l$ becomes equal to $\sigma$) falls on the considered basin whose depth exceeds the thickness of the bottom boundary layer, then existence and uniqueness of the solution are possible, if horizontal turbulent friction is taken into account in the initial dynamics equations [4]. However, in this case we have a higher order equation for the level, and there arise some additional difficulties, due to the fact that we have to set one more boundary condition on the contour of the basin.

In HN-method we do not make any assumptions about the nature of time variations of tidal characteristics. Instead, arbitrary initial conditions are set for tidal oscillations of the level and velocity transport. Integration of the initial system of equations is carried out numerically by stationarity method. A solution is assumed to be found when it becomes periodic, which happens if we set periodic boundary conditions for the level at the open input.

If we do not set periodic conditions, we can consider nonlinear frictional effects. Unfortunately, it is impossible to take accurately into account these and Coriolis effects, because in numerical realization of the method, we use Eliassen's grid. As is known, in this case, one has to make space interpolation which leads to smoothing of fields of tidal elements. Another important feature of Eliassen's grid is that it cannot satisfy a condition of no slipping on a solid contour of the basin. Therefore, when dynamics equations contain terms describing horizontal turbulent friction, the condition of no slipping is replaced with that of slipping. The latter can result in underestimation of tidal energy dissipation in the regions close to the coast and, as a consequence, to distortion of the tidal energy balance in these regions.

During the last three years we have tested the new method of calculating tidal motions in adjacent seas [5]. In the present paper, we give theoretical substantiation of the difference scheme described in [5] and the results of application of the method in various physical and geographical conditions.

## 2. Basic Equations

Let us consider an adjacent sea of small space length, so that we can neglect an effect of tide-generating forces. In such a sea, tidal motions are formed by interaction of such forces as horizontal gradient forces, pressure, Coriolis forces, inertness, bottom and horizontal turbulent friction. Therefore if we apply the usual method of describing macroturbulence in a sea of variable depth, initial tidal dynamics equations can be written as follows:

$$\frac{\partial w}{\partial t} - A\,\Delta w + A_1 w + A_1 w + \frac{r}{D^2}\,|\,w\,|\,w = -gG \operatorname{grad} \zeta, \tag{2.1}$$

$$\frac{\partial \zeta}{\partial t} + \operatorname{div} w = 0, \tag{2.2}$$

where $w$ is vector function with components $u$, $v$, which are the components of total transport along $x$, $y$ axis, $\zeta$ the vertical displacement of the sea level, $D$ the depth, $r$ and $A$ the coefficients of the bottom and horizontal turbulent friction, $g$ the acceleration of gravity, $t$ the time, $A_1$ the matrix of coefficients equal to $\begin{pmatrix} 0 & -l \\ l & 0 \end{pmatrix}$, $l$ the Coriolis parameter, $\Delta$ the plane Laplace operator. $w$ is regarded equal to zero on the coastline $\Gamma_1$,

$$w/\Gamma_1 = 0, \tag{2.3}$$

and a known function of horizontal coordinates and time on the liquid sea boundary $\Gamma_2$,

$$w/\Gamma_2 = a(x, y, t). \tag{2.4}$$

Besides, according to the law of mass conservation, the values of $w_n$ on the contour $\Gamma_2$ must satisfy the following integral relation:

$$\int_0^T dt \int_{\Gamma_2} w_n \, d\Gamma = 0, \tag{2.5}$$

where $w_n$ is a normal component to the liquid boundary $\Gamma_2$ of total transport, $d\Gamma$ is an element of the contour, and $T$ is tidal period.

Let us drop the condition of periodic variations of $w$ and $\zeta$ in time, and turn to a solution of the problem with initial data. It will be supposed that at an initial moment of time (at $t = 0$), fields of tidal currents and of level oscillations are known.

$$w = w_0\,; \qquad \zeta = \zeta_0\,, \qquad \text{with} \quad t = 0, \tag{2.6}$$

where $w_0$, $\zeta_0$ are known functions of horizontal coordinates.

It will be noted here that the quadratic resistance law accepted in (2.1) does not take into account the existing shift of phases between shear stress at the bottom and the tidal current. Another method for calculating the bottom friction without this disadvantage was suggested in [6], where it was shown that the bottom friction coefficient is not a universal constant, but depends in a complex manner on external parameters determining turbulent regime in the bottom boundary layer.

## 3. Difference Scheme

For a numerical solution of the above system of equations (2.1) and (2.2), we use a method of finite differences. For this purpose we use the difference alternating direction scheme proposed in [5], where the system (3.1) of difference equations is written as follows[1]):

$$\frac{u^{n+1/2}-u^n}{\tau}+\frac{1}{2}R_1{}^n u^{n+1/2}=-\frac{1}{2}gD\frac{\partial\zeta^n}{\partial x}-\frac{l}{2}v^n$$
$$-\frac{1}{2}R_1{}^n\tilde{a}_1^{n+1/2}+\frac{A}{2}(u^n_{x\bar x}+u^{n+1/2}_{y\bar y})+\frac{f_1^{n+1/2}}{2}, \tag{3.1$_1$}$$

$$\frac{v^{n+1/2}-v^n}{\tau}+\frac{1}{2}R_1{}^n v^{n+1/2}=-\frac{1}{2}gD\frac{\partial\zeta^n}{\partial y}+\frac{l}{2}u^{n+1/2}$$
$$-\frac{1}{2}R_1{}^n\tilde{a}_2^{n+1/2}+\frac{A}{2}(v^{n+1/2}_{x\bar x}+v^n_{y\bar y})+\frac{f_2^{n+1/2}}{2}, \tag{3.1$_2$}$$

$$\frac{v^{n+1}-v^{n+1/2}}{\tau}+\frac{1}{2}R_1^{n+1/2}v^{n+1}=-\frac{1}{2}gD\frac{\partial\zeta^{n+1}}{\partial y}+\frac{l}{2}u^{n+1/2}$$
$$-\frac{1}{2}R_1^{n+1/2}\tilde{a}_2^{n+1}+\frac{A}{2}(v^{n+1/2}_{x\bar x}+v^{n+1}_{y\bar y})+\frac{f_2^{n+1}}{2}, \tag{3.1$_3$}$$

$$\frac{u^{n+1}-u^{n+1/2}}{\tau}+\frac{1}{2}R_1^{n+1/2}u^{n+1}=-\frac{1}{2}gD\frac{\partial\zeta^{n+1}}{\partial x}-\frac{l}{2}v^{n+1}$$
$$-\frac{1}{2}R_1^{n+1/2}\tilde{a}_1^{n+1}+\frac{A}{2}(u^{n+1}_{x\bar x}+u^{n+1/2}_{y\bar y})+\frac{f_1^{n+1}}{2}, \tag{3.1$_4$}$$

$$\frac{\partial\zeta^{n+1}}{\partial x}=\frac{\partial\zeta^n}{\partial x}-\frac{\tau}{2}(u^{n+1}_{x\bar x}+u^{n+1/2}_{x\bar x}+v^{n+1/2}_{y\bar x}+v^n_{y\bar x}), \tag{3.1$_5$}$$

$$\frac{\partial\zeta^{n+1}}{\partial y}=\frac{\partial\zeta^n}{\partial y}-\frac{\tau}{2}(u^{n+1/2}_{x\bar y}+u^n_{x\bar y}+v^{n+1}_{y\bar y}+v^{n+1/2}_{y\bar y}). \tag{3.1$_6$}$$

Here, for any function $u$, $v$ and the coordinates $x$, $y$,

$$v_x(x,y,t)=(1/h)[v(x+h,y,t)-v(x,y,t)],$$
$$v_{\bar x}(x,y,t)=(1/h)[v(x,y,t)-v(x-h,y,t)],$$
$$v_{x\bar x}=(v_x)_{\bar x},$$

[1] Note: The difference scheme given below is of explicit–implicit character (it is explicit for equations of gradient of the level, and implicit for equations of complete flows).

$\tau$ is a time step, $h$ finite difference grid length, $(\partial\zeta/\partial x)$, $(\partial\zeta/\partial y)$ are components of horizontal gradient of the level, $R_1 = (r/D^2)\sqrt{(u + \tilde{a}_1)^2 + (v + \tilde{a}_2)^2}$, $\tilde{a}_1$, $\tilde{a}_2$ are components of vector $\tilde{a}$, $f_1$ and $f_2$-values depending on $\tilde{a}_1$, $\tilde{a}_2$ and their difference relations along $x$, $y$, and $t$. Since $\tilde{a}_1$ and $\tilde{a}_2$ are sufficiently smooth functions, these difference relations are restricted by modulus.

It will be noted that relations $(3_5)$ and $(3_6)$ for $(\partial\zeta/\partial x)$ and $(\partial\zeta/\partial y)$ are derived by approximation of the continuity equation differentiated with respect to $x$ and $y$[2]).

We add to system (3.1) boundary conditions $u$, $v/\Gamma = 0$ and initial data for $u$, $v$, $(\partial\zeta/\partial x)$, $(\partial\zeta/\partial y)$.

Henceforth, the symbol $\Omega_h$ will denote a set of grid points belonging to the domain $\Omega$ and $\Gamma_h$ its boundary. We introduce also the following notations for the vector $w_h = (u_h, v_h)$:

$$w_h^{\,2} = u_h^{\,2} + v_h^{\,2}, \qquad w_{hx}^2 = u_{hx}^2 + v_{hx}^2, \qquad w_{h\bar{x}}^2 = u_{h\bar{x}}^2 + v_{h\bar{x}}^2 .$$

Besides, we introduce finite difference norm and scalar product according to the formulae

$$\| w_h^{\,k} \|^2 = h^2 \sum_{\Omega_h} (w_h^{\,k})^2,$$

$$\| w_{hx}^{k} \|^2 = h^2 \sum_{\Omega_h} (w_{hx}^{k})^2,$$

$$(f_h^{\,k}, w_h^{\,k}) = h^2 \sum_{\Omega_h} f_h^{\,k} w_h^{\,k},$$

where $\bar{\Omega}_h = \Omega_h \cup \Gamma_h$, subscript $h$ of the function $w_h$ indicates that $w$ is considered in grid points and superscript "$k$" indicates that $w_h$ is taken on the layer $t = k\tau$.

To prove the stability of scheme (3.1), we make use of the following well known relations:

$$2\tau u_{\bar{t}}^{k} u^k = (u^k)^2 - (u^{k-1})^2 + \tau^2 (u_{\bar{t}}^{k})^2, \tag{3.2}$$

$$h^2 \sum_{\Omega_h} u_{hx} v_h = -h^2 \sum_{\Omega_h} u_h v_{h\bar{x}} , \tag{3.3}$$

where

$$u_{\bar{t}}^{k} = \frac{1}{\tau}(u^k - u^{k-1}).$$

Formula (3.3) is valid for the arbitrary functions $u_h$, $v_h$ defined on the grid if $v_h/\Gamma_h = 0$. In order to prove a unique solvability of (3.1), it is sufficient to show

[2] When another method of constructing a difference scheme is used (i.e. when the terms containing grad $\zeta$ and div $w$ are approximated by central differences), then in determining the level $\zeta$ on the grid boundary, $\Gamma_h$ it is necessary to set velocity components at grid points outside of the domain $\Omega_h$.

that a homogeneous system corresponding to it on each layer $t = (k/2)\,\tau$, $k = 1, 2, \ldots, (T/\tau)$ has but a trivial solution. Let us multiply homogeneous equations corresponding to ($3_3$) and ($3_4$) by $h^2 \cdot u^{n+1}$ and $h^2 \cdot v^{n+1}$, and sum up the resulting expressions over all grid points, making use of expression (3.3). This yields

$$\| v^{n+1} \|^2 + \tau h^2 \sum_{\Omega_h} R_1^{n+1/2} (v_h^{n+1})^2 + \frac{A\tau}{2} \| v_y^{n+1} \|^2 + \frac{1}{2} g\tau^2 \sum_{\Omega_h} D(v_y^{n+1})^2$$
$$= -\frac{1}{4} g\tau^2 \sum_{\Omega_h} v_y^{n+1} v^{n+1} D_y\,, \tag{3.4}$$

$$\| u^{n+1} \|^2 + \tau h^2 \sum_{\Omega_h} R_1^{n+1/2} (u_h^{n+1})^2 + \frac{A\tau}{h^2} \| u_x^{n+1} \|^2 + \frac{l\tau}{2} (v^{n+1}, u^{n+1}) + \frac{1}{4} g\tau^2 \sum_{\Omega_h} D(u_x^{n+1})^2$$
$$= -\frac{1}{4} g\tau^2 \sum_{\Omega_h} u_x^{n+1} u^{n+1} D_x\,. \tag{3.5}$$

From the above relations follow the inequalities

$$\| v^{n+1} \|^2 + \frac{A\tau}{2} \| v_y^{n+1} \|^2 \leqslant \frac{1}{16} g\tau^2 \lambda_1^{-1} M_1^{\,2} \| v^{n+1} \|^2, \tag{3.6}$$

$$\| u^{n+1} \|^2 + \frac{A\tau}{2} \| u_x^{n+1} \|^2 \leqslant \frac{1}{16} g\tau^2 \lambda_1^{-1} M_1^{\,2} \| u^{n+1} \|^2 + \frac{l\tau}{2} \| v^{n+1} \| \| u^{n+1} \|, \tag{3.7}$$

where

$$M_1 = \max_{\Omega_h} \{D_{hx}, D_{hy}\}, \qquad \lambda = \min_{\Omega_h} D_h\,.$$

If $\tau (\tau < 4\sqrt{\lambda_1/g}\, M_1^{-1})$ is sufficiently small, from (3.6) and (3.7) it follows that $\| v^{n+1} \| = \| u^{n+1} \| = 0$. In this case, employing the equations for $(\partial\zeta/\partial x)$ and $(\partial\zeta/\partial y)$, we find that $(\partial\zeta/\partial x)$ and $(\partial\zeta/\partial y)$ are equal to zero in the whole domain $\Omega_h$.

Thus, we have proved that a homogeneous system has but a trivial solution, and, hence, that an inhomogeneous system is uniquely solvable for any right side[3]).

*Stability of the Difference Scheme* (3.1)

Let us prove stability of the difference scheme (3.1). For definiteness it will be assumed that at an initial moment components of transport $u$, $v$ and those of the level's horizontal grandients $(\partial\zeta/\partial x)$ and $(\partial\zeta/\partial y)$ are equal to zero[4].

[3] Note: in the case of a uniform depth $D$ (i.e., when $M_1 = 0$), system (3.1) can be uniquely solved for any $\tau$.

[4] Nonzero initial conditions will add (during conversion) the terms which can be included in the addends denoted by symbol $f$.

Let us multiply $(3_1)$, $(3_2)$, $(3_3)$, $(3_4)$ by $2\tau h^2 u^{n+1/2}$, $2\tau h^2 v^{n+1/2}$, and $2\tau h^2 u^{n+1}$, respectively, and sum up the resulting expressions over all points $\Omega_h$. Then we add expressions one and two and expressions three and four. Employing formulae (3.2) and (3.3), and an easily verifiable expression

$$A\tau(u_x{}^k, u_x^{k+1/2}) = A\tau \| u_x^{k+1/2} \|^2 - A\tau^2(u_{x\bar{t}}^{k+1/2}, u_x^{k+1/2}), \tag{3.8}$$

$$k = 0, \tfrac{1}{2}, 1, \ldots,$$

we get the basic energy identity

$$\| w^{n+1} \|^2 - \| w^n \|^2 + \tau^2(\| w_{\bar{t}}^{n+1/2} \|^2 + \| w_{\bar{t}}^{n+1} \|^2)$$

$$+ A\tau\{\| w_x^{n+1/2} \|^2 + \| w_x^{n+1} \|^2 + \| w_y^{n+1/2} \|^2 + \| w_y^{n+1} \|^2\} + (B^{n+1/2})^2 + (B^{n+1})^2$$

$$= T^{n+1} + A\tau^2\{(u_{y\bar{t}}^{n+1/2}, u_y^{n+1/2}) + (v_{x\bar{t}}^{n+1/2}, v_x^{n+1/2}) + (u_{x\bar{t}}^{n+1}, u_x^{n+1}) + (v_{y\bar{t}}^{n+1}, v_y^{n+1})\}$$

$$+ B_1^{n+1/2} + B_1^{n+1}, \tag{3.9}$$

where

$$u_{\bar{t}}^{k+1/2} = \frac{1}{\tau}(u^{k+1/2} - u^k),$$

$$(B^{k+1/2})^2 = \tau h^2 \sum_{\Omega_h} R_1{}^k[(u_n^{k+1/2})^2 + (v_h^{k+1/2})^2],$$

$$B_1^{k+1/2} = \tau\{l(u^{k+1/2}, v^{k+1/2} - v^k) + (f^{k+1/2}, w^{k+1/2})$$

$$- (R_1{}^k\tilde{a}_1^{k+1/2}, u^{k+1/2}) - (R_1{}^k\tilde{a}_2^{k+1/2}, v^{k+1/2})\},$$

$$k = n, n + \tfrac{1}{2};$$

$$T^{n+1} = -g\tau\left[\left(D\frac{\partial\zeta^n}{\partial x}, u^{n+1/2}\right) + \left(D\frac{\partial\zeta^n}{\partial y}, v^{n+1/2}\right)\right.$$

$$\left. + \left(D\frac{\partial\zeta^{n+1}}{\partial x}, u^{n+1}\right) + \left(D\frac{\partial\zeta^{n+1}}{\partial y}, v^{n+1}\right)\right].$$

The second term in the right side of (3.8) is found as follows:

$$A\tau^2 |(u_{x\bar{t}}^{k+1/2}, u_x^{k+1/2})| \leqslant \frac{2A^2\tau^2}{h^2} \| u_x^{k+1/2} \|^2 + \frac{\tau^2}{2} \| u_{\bar{t}}^{k+1/2} \|^2,$$

$$k = n, n + \tfrac{1}{2}. \tag{3.10}$$

The last summand in (3.9) is found like this:

$$\begin{aligned}|B_1^{k+1/2}| &\leqslant \frac{\tau}{2}\{\epsilon_1^2 \| w^{k+1/2} \|^2 + \epsilon_1^{-2} \| f^{k+1/2} \|^2 \\ &+ |l| (\| w^{k+1/2} \|^2 + \| w^k \|^2) + \tfrac{1}{2}\epsilon_2^2 \| w^{k+1/2} \|^2 \\ &+ \tfrac{1}{2}\epsilon_2^{-2} \| a^{k+1/2} \|^2 + r\lambda_1^{-2}[\max_{\Omega_h} | a^{k+1/2} | (\| w^{k+1/2} \|^2 + \| w^k \|^2)]\} \\ &\equiv C\tau(\| w^{k+1/2} \|^2 + \| w^k \|^2) + C_1, \qquad k = n, n + \tfrac{1}{2},\end{aligned} \tag{3.11}$$

where $\epsilon_1$, $\epsilon_2$ are any positive quantities, $C$ and $C_1$ constants depending on the choice of $\epsilon_1$, $\epsilon_2$ and conditions of the problem.

Let

$$\begin{aligned}b^n &= u_x{}^n + v_y{}^n, \\ b^{n+1/2} &= u_x^{n+1/2} + v_y^{n+1/2}, \\ L_n &= \sum_{k=0}^{n} b^k + \sum_{k=0}^{n-1} b^{k+1/2}, \\ L^{n+1/2} &= \sum_{k=0}^{n} b^k + \sum_{k=0}^{n} b^{k+1/2},\end{aligned}$$

and indices "$D$" and "$D_x$" of any vector $\{v_h\}$ indicate that instead of $\{v_h\}$ we consider vectors $\{v_h \sqrt{D_h}\}$ and $\{v_h D_{hx}\}$, respectively.

Using relations $(3.1_5)$, $(3.1_6)$, (3.2), and (3.3) we rewrite the first term in the right side of (3.9):

$$T_\zeta^{n+1} = -\frac{g\tau^2}{2}(T_1^{n+1} + T_2^{n+1}), \tag{3.12}$$

where

$$\begin{aligned}T_1^{n+1} &= (L_D^{n+1}, b_D^{n+1} - b_D^{n+1/2}) - (b_D^{n+1}, b_D^{n+1/2}) - \| b_D^{n+1/2} \|^2 \\ &- (v_{yD}^{n+1}, u_{xD}^{n+1/2}) - (u_{xD}^{n+1}, v_{yD}^{n+1/2}) - 2(v_{yD}^{n+1}, u_{xD}^{n+1}), \\ T_2^{n+1} &= (L^{n+1}, u_{D_x}^{n+1/2}) + (L^{n+1}, u_{D_x}^{n+1}) + (L^{n+1}, v_{D_y}^{n+1/2} + v_{D_y}^{n+1}) \\ &- (b^{n+1} + v_y{}^n + b^{n+1/2}, u_{D_x}^{n+1/2}) - (b_1^{n+1} + u_x{}^n + b^{n+1/2}, v_{D_y}^{n+1/2}) \\ &- (v_y^{n+1}, u_{D_x}^{n+1}) - (u_x^{n+1}, v_{D_y}^{n+1}).\end{aligned}$$

Summing up the above equality over $k$ through 0 to $n$, we get

$$\sum_{k=0}^{n} T_{\zeta}^{k+1} = -\frac{g\tau^2}{4}\Big[\| L_D^{n+1} \|^2 + \sum_{k=0}^{n} (s^{k+1} + 2T_2^{k+1})\Big], \tag{3.13}$$

where

$$s^{k+1} = \| u_{xD}^{k+1} - v_{yD}^{k+1} \|^2 - \| b^{k+1/2} \|^2 - 2(v_y^{k+1}, u_x^{k+1/2}) - 2(u_x^{k+1}, v_y^{k+1/2}).$$

For $| T_2^{k+1} |$ the following estimate is valid:

$$\frac{g\tau^2}{2} | T_2^{k+1} | \leqslant M_1\tau^3 \sqrt{\frac{g}{\lambda_1}}\, g \| L_D^{k+1} \|^2 + M_1\tau \sqrt{\frac{g}{\lambda_1}} (\| w^{k+1} \|^2 + \| w^{k+1/2} \|^2)$$
$$+ \frac{5g\tau^2 M_1}{h} (\| w^{k+1} \|^2 + \| w^{k+1/2} \|^2). \tag{3.14}$$

Let the following condition be fulfilled:

$$\frac{A\tau}{h^2} < 1. \tag{3.15}$$

Then, after summing up relations (3.9) over $k$ through 0 to $n$, and considering expressions (3.10)–(3.14) and the estimates appearing in $s^k$ of difference derivatives in terms of the functions $u$, $v$, we get the following a priori estimate:

$$\| y^{n+1} \|^2 \leqslant \Big(\frac{2g \max_{\Omega_h} D_h \tau^2}{h^2} + C_2(\epsilon_1, \epsilon_2, r, l)\tau$$
$$+ M_1\tau \sqrt{\frac{g}{\lambda_1}} + \frac{5g\tau^2 M_1}{h}\Big) \sum_{k=0}^{n} (\| y^{k+1} \|^2 + \| y^{k+1/2} \|^2) + C_3, \tag{3.16}$$

where

$$\| y^{n+1} \|^2 = \| w^{n+1} \|^2 + g \| L_D^{n+1} \|^2,$$
$$\| y^{n+1/2} \|^2 = \| w^{n+1/2} \|^2 + g \| L_D^{n+1/2} \|^2, \; C_2, C_3$$

are constants joining all constants in corresponding estimates.

A similar inequality is valid, beginning with the layer $t = (n + \frac{1}{2})\tau$,

$$\| y^{n+1/2} \|^2 \leqslant \Big(\frac{2g \max_{\Omega_h} D_h{}^2 \tau^2}{h^2} + C_2(\epsilon_1, \epsilon_2, r, l)\tau$$
$$+ M_1\tau \sqrt{\frac{g}{\lambda_1}} + \frac{5g\tau^2 M_1}{h}\Big) \sum_{k=0}^{n} (\| y^k \|^2 + \| y^{k+1/2} \|^2 + C_4. \tag{3.16'}$$

Let us require that, in addition to (3.15), the following condition be fulfilled, too:

$$\frac{2g \max_{\Omega_h} D_h \tau^2}{h^2} + C_2\tau + M_1\sqrt{\frac{g}{\lambda_1}}\,\tau + \frac{5g\tau^2 M_1}{h} < 1. \tag{3.17}$$

Then, considering the fact that (3.16) and (3.16′) are difference approximations of the differential inequality

$$\frac{dz}{dt} \leqslant C_5(t)z + C_6(t)$$

with $z = \int_0^t \| w \|^2 + g \| L_D \|^2)\, dt$, and using the finite difference analog of Lemma 1 in [7], we derive, on the basis of (3.16) and (3.16′), the following expression:

$$\| y^k \| \leqslant C_7, \qquad k = n; \qquad n + \tfrac{1}{2}; \qquad n = 0, 1,..., N = (T/\tau), \tag{3.18}$$

which ensures stability of the difference scheme (3.1) if conditions (3.15) and (3.17) are fulfilled. In (3.18), $C_7$ is a constant independent of $k$.

It will be remarked that with $D(x) = D_0 = \text{const.}$, condition (3.17) can be reduced to[5]

$$\frac{2gD_0\tau^2}{h^2} + C_2(\epsilon_1, \epsilon_2, r, l)\tau < 1. \tag{3.19}$$

Because of smallness of $C_2$ for small values of $\epsilon_1$, $\epsilon_2$, $r$, $l$, from (3.19) follows the Courant–Friedrichs–Levy criterion

$$\frac{2gD_0\tau^2}{h^2} < 1. \tag{3.20}$$

Fulfilment of condition (3.15), with $\tau$, $h \to 0$, naturally, involves fulfilment of (3.17) or (3.20). Therefore, one can take just one condition, (3.15), as stability criterion for scheme (3.1). However, in concrete calculations, when $\tau$ and $h$ take on fixed values, conditions (3.15) and (3.17) both should be checked.

## *Convergence*

In order to prove convergence of the difference solution $\mathfrak{w}_h$, $\zeta_h$ to a solution of problems (2.1)–(2.3), it will be supposed that problems (2.1)–(2.3) have a sufficiently smooth solution $\mathfrak{w}^*(\underline{x}, t)$, $\zeta^*(\underline{x}, t)$. Let $\mathfrak{w}_h^*$, $(\partial\zeta^*/\partial x)_h$, $(\partial\zeta^*/\partial y)_h$ correspond on the grid with $\mathfrak{w}^*$, $(\partial\zeta^*/\partial x)$, $(\partial\zeta^*/\partial y)$. Equalities (3.1) are correct for $\mathfrak{w}_h^*$, $(\partial\zeta^*/\partial x)_h$,

[5] For the wave components with a minimal possible wavelength equal to $2h$, a condition of stability equivalent to (3.19) was obtained in [8]. A general analysis of the dispersity equation corresponding to the linearized system (3.1) with constant coefficients is given in [5].

$(\partial\zeta^*/\partial y)_h$ with discrepancies to be denoted as $r_1{}^m$, $r_2{}^m$, $\rho_1{}^m\rho_2{}^m$, respectively. These discrepancies vanish if $\tau$, $h \to 0$, when the solution $\underline{w}^*$, $\zeta^*$ is sufficiently smooth (e.g., when all functions and their derivatives appearing in the initial system are continuous).

For

$$p_h = \underline{w}_h - \underline{w}_h{}^*, \qquad \rho_{1h} = \left(\frac{\partial\zeta}{\partial x}\right)_h - \left(\frac{\partial\zeta^*}{\partial x}\right)_h,$$

$q_{2h} = (\partial\zeta/\partial y)_h - (\partial\zeta^*/\partial y)_h$, we can write the following difference system:

$$\begin{aligned}\frac{p_1^{n+1/2} - p_1{}^n}{\tau} &+ \frac{r}{2D^2}\,|\,\underline{p}^n + \underline{w}^{*n}\,|\,p_1^{n+1/2}\\ &= -\frac{gD}{2}\,q_1{}^n + \frac{A}{2}\,(p_{1x\bar{x}}^n + p_{1y\bar{y}}^{n+1/2}) - \frac{l}{2}\,p_2{}^n + r_1^{n+1/2}\\ &\quad - \frac{r}{2D^2}\,u^{*n+1/2}(|\,\underline{p}^n + \underline{w}^{*n}\,| - |\,\underline{w}^{*n}\,|),\end{aligned} \tag{3.21$_1$}$$

$$\begin{aligned}\frac{p_2^{n+1/2} - p_2{}^n}{\tau} &+ \frac{r}{2D^2}\,|\,\underline{p}^n + \underline{w}^{*n}\,|\,p_2^{n+1/2}\\ &= -\frac{gD}{2}\,q_2{}^n + \frac{A}{2}\,(p_{2x\bar{x}}^{n+1/2} + p_{2y\bar{y}}^n) + \frac{l}{2}\,p_1^{n+1/2} + r_2^{n+1/2}\\ &\quad - \frac{r}{2D^2}\,v^{*n+1/2}(|\,\underline{p}^n + \underline{w}^{*n}\,| - |\,\underline{w}^{*n}\,|),\end{aligned} \tag{3.21$_2$}$$

$$\begin{aligned}\frac{p_2^{n+1} - p_2^{n+1/2}}{\tau} &+ \frac{r}{2D^2}\,|\,\underline{p}^{n+1/2} + \underline{w}^{*n+1/2}\,|\,p_2^{n+1}\\ &= -\frac{gD}{2}\,q_2^{n+1} + \frac{A}{2}\,(p_{2x\bar{x}}^{n+1/2} + p_{2y\bar{y}}^{n+1}) + \frac{l}{2}\,p_1^{n+1/2} + r_2^{n+1}\\ &\quad - \frac{r}{2D^2}\,v^{*n+1}(|\,\underline{p}^{n+1/2} + \underline{w}^{*n+1/2}\,| - |\,\underline{w}^{*n+1/2}\,|),\end{aligned} \tag{3.21$_3$}$$

$$\begin{aligned}\frac{p_1^{n+1} - p_1^{n+1/2}}{\tau} &+ \frac{r}{2D^2}\,|\,\underline{p}^{n+1/2} + \underline{w}^{*n+1/2}\,|\,p_1^{n+1}\\ &= -\frac{gD}{2}\,q_1^{n+1} + \frac{A}{2}\,(p_{1x\bar{x}}^{n+1} + p_{1y\bar{y}}^{n+1/2}) - \frac{l}{2}\,p_2^{n+1} + r_1^{n+1}\\ &\quad - \frac{r}{2D^2}\,u^{*n+1}(|\,\underline{p}^{n+1/2} + \underline{w}^{*n+1/2}\,| - |\,\underline{w}^{*n+1/2}\,|),\end{aligned} \tag{3.21$_4$}$$

$$q_2^{n+1} = q_2{}^n - \frac{\tau}{2}\,(p_{1x\bar{y}}^{n+1/2} + p_{1x\bar{y}}^n + p_{2y\bar{y}}^{n+1} + p_{2y\bar{y}}^{n+1/2}) + \tau\rho_2^{n+1}, \tag{3.21$_5$}$$

$$q_1^{n+1} = q_1{}^n - \frac{\tau}{2}\,(p_{1x\bar{x}}^{n+1} + p_{1x\bar{x}}^{n+1/2} + p_{2y\bar{x}}^{n+1/2} + p_{2y\bar{x}}^{n+1/2}) + \tau\rho_1^{n+1}. \tag{3.21$_6$}$$

In order to reduce calculations, it will be supposed that $\Gamma_h = \Gamma$. Then boundary conditions for $p_h$ can be presented in a form $p_h/\Gamma_h = 0$.

Let us multiply each equation of (3.21) by $2\tau h^2$ and a corresponding function, and then sum up the resulting expressions over the whole domain $\Omega_h$. After conversions identical to those made in proving stability, we get inequalities which differ from (3.16) and (3.16′) only in additional terms, i.e.,

$$\| y^{n+1} \|^2 \leqslant C_8 \tau \sum_{k=0}^{n} (\| y^{k+1} \|^2 + \| y^{k+1/2} \|^2) + j^{n+1}, \tag{3.22}$$

$$\| y^{n+1/2} \|^2 \leqslant C_9 \tau \sum_{k=0}^{n} (\| y^{k} \|^2 + \| y^{k+1/2} \|^2) + j^{n+1/2}. \tag{3.22′}$$

Here $\| y^{n+1} \|$, $y^{n+1/2} \|$ are found, analogously to (3.16), (3.16′), by substituting $p_h$ for $w_h$:

$$j^{n+1} = \tau \left[ \sum_{k=0}^{n+1} (\underline{r}^k, p^k) + \sum_{k=0}^{n} (\underline{r}^{k+1/2}, p^{k+1/2}) \right]$$

$$+ g \max_{\Omega_h} D_h \tau^2 \sum_{k=0}^{n} \sum_{i=0}^{k} (\rho^i, \rho^i),$$

$$j^{n+1/2} = \tau \left[ \sum_{k=0}^{n} (\underline{r}^k, p^k) + \sum_{k=0}^{n} (\underline{r}^{k+1/2}, p^{k+1/2}) \right]$$

$$+ g \max_{\Omega_h} D_h \tau^2 \sum_{k=0}^{n} \sum_{i=0}^{k} (\rho^i, \rho^i),$$

$\underline{r}$ and $\rho$ being vectors with components $\binom{r_1}{r_2}$ and $\binom{\rho_1}{\rho_2}$, respectively.

Modulus $j^{n+1}$ will be found as follows:

$$| j^{n+1} | \leqslant C_{10} \tau \sum_{k=0}^{n} (\| p^{k+1} \|^2 + \| p^{k+1/2} \|^2) + j_1^{n+1},$$

where

$$j_1^{n+1} = C_{11} \tau \sum_{k=0}^{n} (\| \underline{r}^{k+1} \|^2 + \| \underline{r}^{k+1/2} \|^2 + \| \rho^k \|^2).$$

Similarly, we find $| j^{n+1/2} |$. By means of inequalities (3.22) and (3.22′), if $\tau(\tau < \frac{1}{2}(\max(C_8, C_9) + C_{10}))$ is sufficiently small, we find the estimate $\| y^k \|$ in terms of $j_1{}^k$

$$\| y^k \| \leqslant C_{12} j_1{}^k, \qquad k = n, n + \frac{1}{2}; \qquad n = 0, 1, \ldots, N = \frac{T}{\tau}.$$

Assuming smoothness of a solution, we get $j_1^k \to 0$ if $\tau, h \to 0$. From here follows convergence of the difference solution $w_h$, $(\partial\zeta/\partial x)_h$, $(\partial\zeta/\partial y)_h$ to $w^*$, $(\partial\zeta^*/\partial x)(\partial\zeta^*/\partial y)$ in difference norm.

Hence, we have proved convergence of the difference scheme (3.1).

An assumption of correspondence of $\Gamma_h$ with $\Gamma$ can be changed for a requirement of smoothness of $\Gamma$.

Using the methods described in [9, 10] one can prove convergence of the difference solution $w_h$, $\zeta_h$ with the solution $w^* \in \underline{W}_2^2(\Omega) \cap \overset{\circ}{\underline{W}}_2^1(\Omega)$, $\zeta^* \in L_2(\Omega)$ for any $t \in [0, T]$.

## 4. Results of Application of the Method

The method described here was tested in the North Sea and in four regions of the Arctic Seas, to be referred to as regions $A$, $B$, $C$, $D$. We have chosen these basins because, first, they are studied in more detail as regards tides and, second, because of a variety of conditions that cause tidal motions in these basins. Thus, here there are various forms of the bottom relief, a variety of sea lengths and coastline shape. Besides, it is essential that some basins are located in the region of "critical" latitude.

First of all, we shall give a brief account of the procedure by which we determined depths and velocity of tidal current in grid points. Depths were taken from bathymetric charts in points that are spaced half of a mesh size apart. Then, by smoothing over five points, we calculated depths in grid points. Results of numerical experiments showed that such a procedure ensured sufficient smoothing of the bottom relief in the considered regions. A two- or three-fold smoothing did not practically change the results of calculation.

The necessary direction and velocity of the tidal current in points of the liquid contour were determined from hourly charts of the tidal current in the surface layer. The charts were made from observational data. In points of the liquid contour where such data were not available, the direction and velocity of the tidal current were found by interpolation of their values in neighboring grid points.

The mesh length in the North Sea was taken equal to 74 km., in the Arctic basins 50 km.; the time interval in both cases was 12 min. Coefficients of the bottom and horizontal turbulent friction in the considered regions were assumed to be fixed, and equal to $3 \cdot 10^{-3}$, $10^8$ cm²/sec. (in the North Sea) and $3 \cdot 10^{-3}$, $8.5 \cdot 10^8$ cm²/sec. (in the Arctic basins), respectively. These values were chosen by performing a series of experiments in such a way that an error in calculating velocity of the tidal current in check points was minimal.

We present results of comparison of the calculated values of tidal characteristics with the data of factual measurements.

In Fig. 1 is shown a chart of isoamplitudes and co-tidal lines of the main lunar

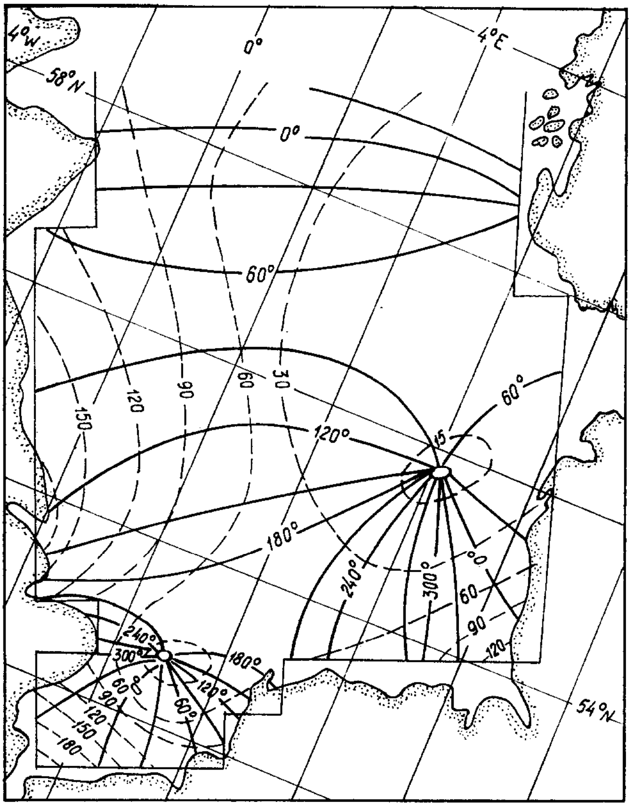

FIG. 1. A chart of isoamplitudes and co-tidal lines of wave $M_2$ in the North Sea.

semidiurnal wave $M_2$ in the North Sea. First of all, it strikes one that the pattern of tidal oscillations we have got is very close to that obtained in [1] on the basis of all available observational data.

We show in Table I a comparison of calculated and observed amplitudes and phases of the level's tidal oscillations in 29 points of the North Sea coast. The table also presents relative errors in calculation of amplitudes in per cent and errors in calculation of phases per hour. One can see that, in most cases, there is a satisfactory agreement between calculated and observed data. Fairly large disagreement observed at Hunstanton Pier, Cromer, and Delfzijl seems to be due to local peculiarities of the sea bottom relief and of the coastline configuration, which could not be considered in calculations.

Analysis of Figs. 2 and 3, which illustrate calculated and observed data of velocity vector of tidal current for wave $M_2$ in the four regions of the Arctic Seas, shows

Table I

A Comparison of Calculated and Observed Tidal Oscillations of the Level in Different Points of the North Sea Coast

| | | Coordinates | | Amplitudes (cm) | | | Phase (dg) | | |
|---|---|---|---|---|---|---|---|---|---|
| N° | Name of point | Latitude | Longitude | Calc. | Obs. | Rel. err. % | Calc. | Obs. | Calc. error per hour |
| 1 | 2 | 3 | 4 | 5 | 6 | 7 | 8 | 9 | 10 |
| 1 | Aberdeen | 57°09′ | 2°05′ W | 113 | 131 | 21 | 30 | 25 | 0.17 |
| 2 | Arbroath | 56°03′ | 2°35′ W | 130 | 155 | 16 | 65 | 44 | 0.7 |
| 3 | Dunbar | 56°00′ | 2°31′ W | 147 | 161 | 9 | 75 | 56 | 0.6 |
| 4 | Blyth | 55°07′ | 1°21′ W | 160 | 160 | 0 | 87 | 87 | 0.0 |
| 5 | R. Tyne Entrance | 55°01′ | 1°24′ W | 165 | 158 | 4 | 90 | 91 | 0.03 |
| 6 | R. Tees Entrance | 54°36′ | 1°10′ W | 170 | 169 | 1 | 100 | 98 | 0.07 |
| 7 | Whitby | 54°29′ | 0°37′ W | 175 | 165 | 6 | 105 | 103 | 0.07 |
| 8 | Skegness | 53°09′ | 0°21′ E | 150 | 213 | 30 | 180 | 169 | 0.37 |
| 9 | Hunstanton Pier | 52°56′ | 0°29′ E | 130 | 218 | 40 | 204 | 180 | 0.80 |
| 10 | Cromer | 52°56′ | 1°18′ E | 105 | 159 | 34 | 235 | 189 | 1.54 |
| 11 | Winterton | 52°43′ | 1°41′ E | 86 | 102 | 16 | 233 | 211 | 0.74 |
| 12 | Lowestoft | 52°29′ | 1°46′ E | 75 | 70 | 7 | 285 | 259 | 0.87 |
| 13 | Harwich | 51°57′ | 1°17′ E | 138 | 130 | 6 | 325 | 326 | 0.03 |
| 14 | Southend | 51°31′ | 0°45′ E | 185 | 201 | 8 | 326 | 354 | 0.93 |
| 15 | Ramsgate | 51°20′ | 1°25′ E | 197 | 187 | 5 | 340 | 342 | 0.07 |
| 16 | Oostend | 51°14′ | 2°55′ E | 185 | 180 | 1 | 10 | 5 | 0.17 |
| 17 | Zeebrügge | 51°20′ | 3°12′ E | 157 | 169 | 7 | 20 | 15 | 0.17 |
| 18 | Vlissingen | 51°27′ | 3°36′ E | 135 | 172 | 22 | 35 | 32 | 0.10 |
| 19 | Brouwershaven | 51°44′ | 3°54′ E | 98 | 115 | 15 | 55 | 57 | 0.07 |
| 20 | Hoek van Holland | 51°59′ | 4°07′ E | 79 | 80 | 1 | 60 | 64 | 0.13 |
| 21 | Katwijk | 52°12′ | 4°24′ E | 76 | 68 | 12 | 89 | 81 | 0.27 |
| 22 | Ijmuiden | 52°28′ | 4°35′ E | 65 | 68 | 4 | 110 | 106 | 0.13 |
| 23 | Der Helder | 52°58′ | 4°45′ E | 55 | 53 | 4 | 169 | 159 | 0.33 |
| 24 | West Terschelling | 52°22′ | 5°13′ E | 58 | 69 | 16 | 212 | 222 | 0.53 |
| 25 | Delfzijl | 53°20′ | 6°56′ E | 85 | 125 | 32 | 260 | 308 | 1.60 |
| 26 | Helgoland | 54°11′ | 7°53′ E | 95 | 99 | 4 | 330 | 316 | 0.47 |
| 27 | Roter sand Leuchtturm | 53°51′ | 8°05′ E | 118 | 129 | 9 | 328 | 316 | 0.40 |
| 28 | Esbjerg | 55°29′ | 8°28′ E | 54 | 60 | 10 | 30 | 39 | 0.30 |
| 29 | Lister | 58°06′ | 6°36′ E | 7 | 4 | 75 | 58 | 51 | 0.23 |

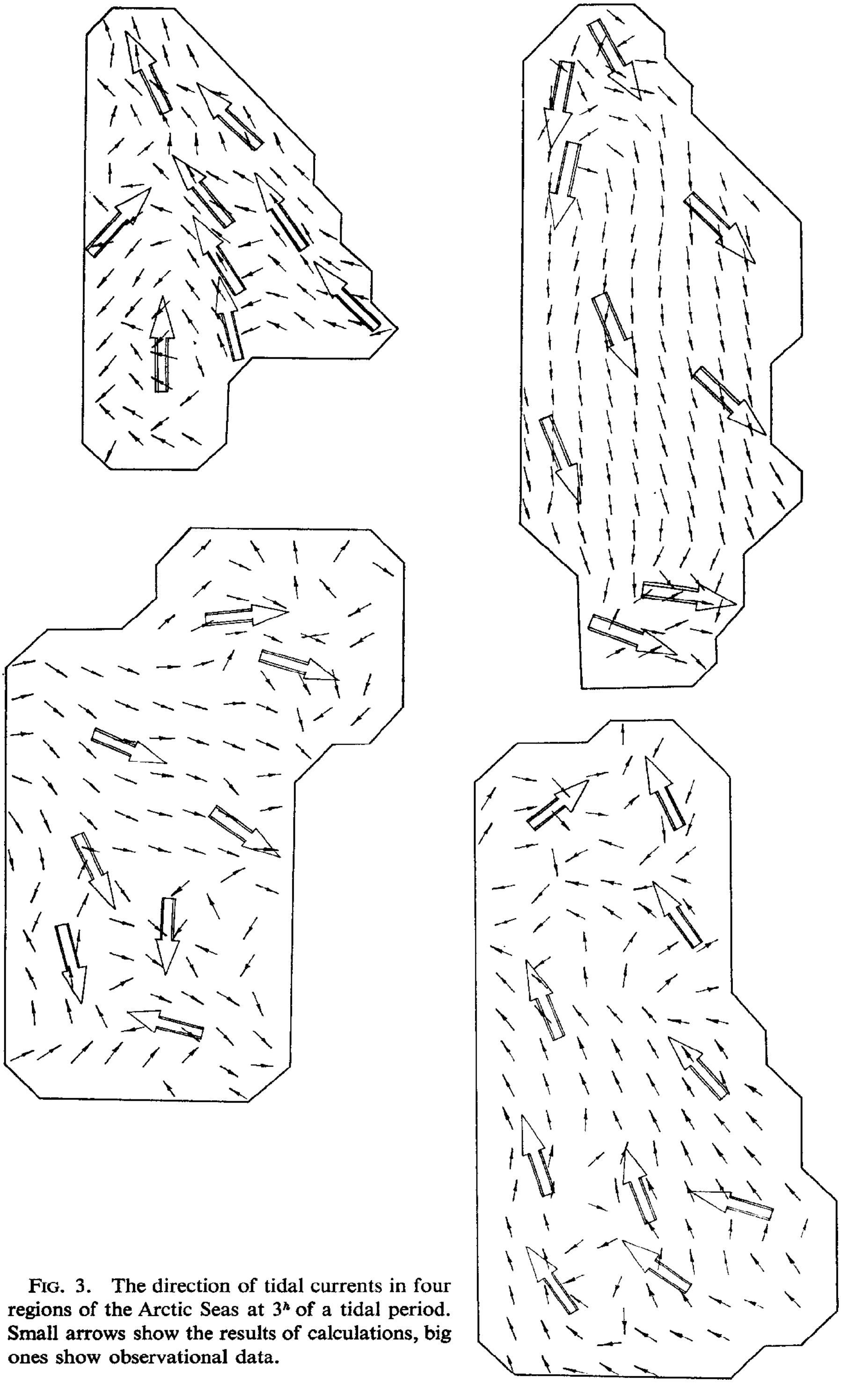

FIG. 3. The direction of tidal currents in four regions of the Arctic Seas at $3^h$ of a tidal period. Small arrows show the results of calculations, big ones show observational data.

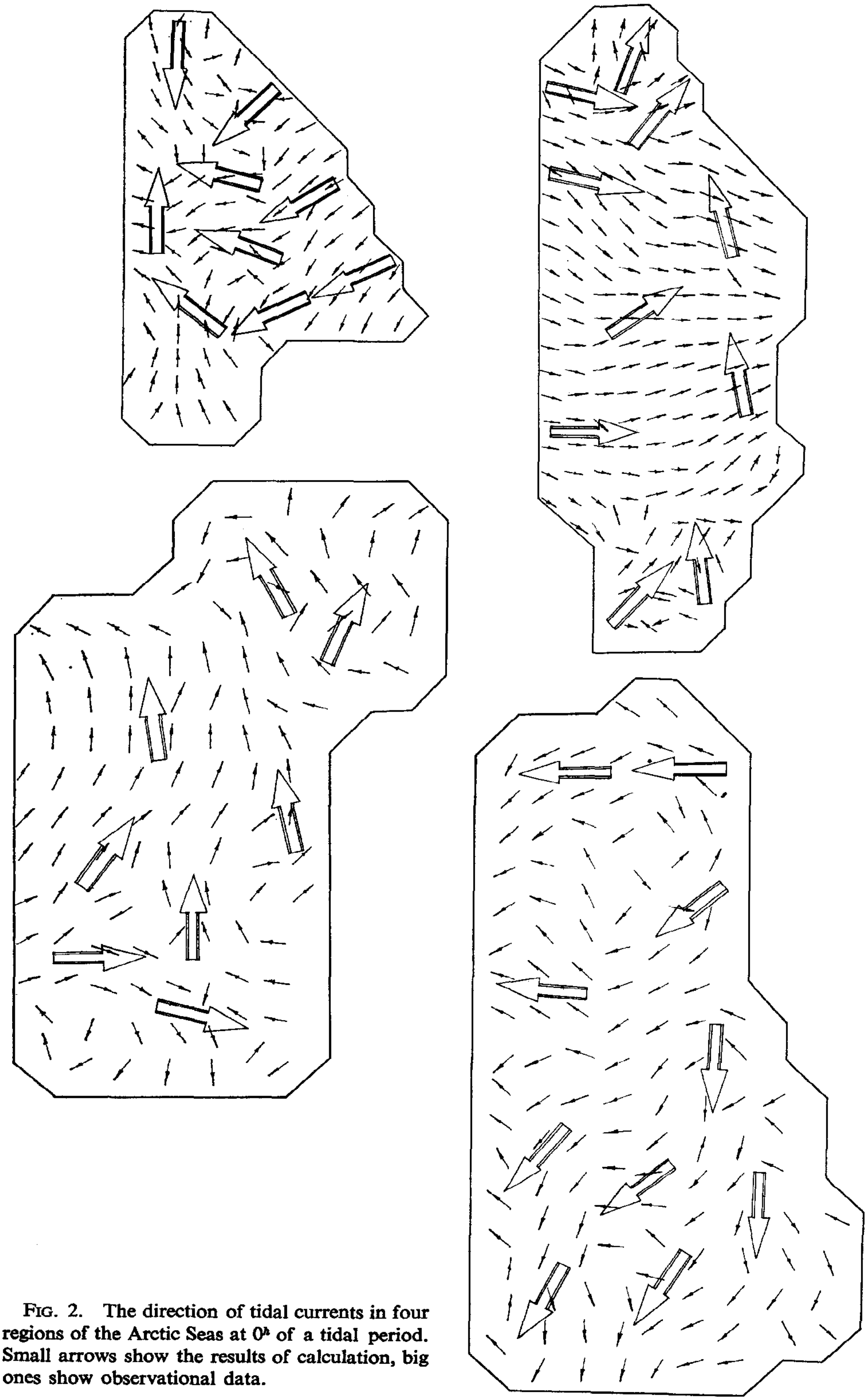

that disagreement between calculated and observed data is, as a rule, not too large in central parts of the considered regions, and it increases in the areas close to the coast. This regularity is especially notable in region $C$, in whose western part disagreement between calculated and observed characteristics of the current

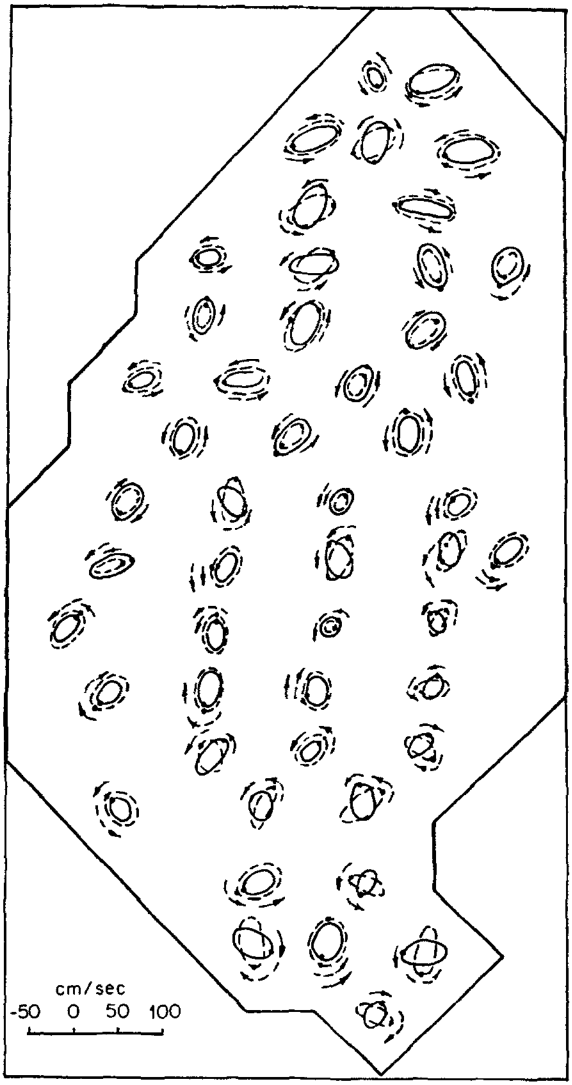


FIG. 4. Ellipses of the tidal current calculated with the help of two resistance laws. See the text for explanation.

appears to be the greatest. According to take-off data, here there is a notable increase in the velocity of tidal current, due to some peculiarities of the bottom relief which have not been considered because their horizontal scale does not exceed the mesh size.

Another reason for essential disagreement between calculated and observed values of the velocity in the sea areas close to the coast might be errors of observations and of the analysis. These errors become especially appreciable with low velocities of tidal currents typical of the Arctic Seas.

It is not excepted, however, that some responsibility ought to be placed upon the method itself, in which some assumptions have been made (such as those associated with the use of fixed values for the coefficients of bottom and horizontal turbulent friction within the considered water basins). In this context, of some interest is Fig. 4, which shows ellipses of tidal current for wave $M_2$ calculated with regard to the dependence of the bottom friction coefficient on the external parameters of the bottom boundary laryer (see [6]), and, consequently, on horizontal coordinates. In the same figure, the dashed line shows ellipses of tidal current obtained with the help of the well known quadratic resistance law. One can see that there is very little difference between the results of the two calculations. This may be due to the presence of large depths in the main part of the considered region, when the bottom friction does not exert any essential influence upon formation of tidal motions.

Southern and southwestern parts of the water basin near the mainland are most representative from the point of view of comparison of the two resistance laws. Here the sea depth is of the order of several tens of meters, and the effect of the friction is essential. Even at a first glance at this figure one can see a striking difference between the tidal current ellipses.

In spite of the restrictions mentioned above, application of the method suggested in [5] for calculation of tidal motions in different physical and geographical conditions proved to be worthwhile. The charts of isoamplitudes and co-tidal lines, as well as the charts of tidal currents, made on the basis of the computed results are, generally speaking, in good agreement with observational data, which allows us to recommend this method for performing mass calculations.

## REFERENCES


1. W. HANSEN, Gezeiten und Gezeitenströme der halbtägigen Hauptmondtide $M_2$ in der Nordsee, Deutsch Hydr. Zeitschr. Ergänzungsheft, **1** (1952), 1–46.
2. W. HANSEN, Theorie zur Errechnung des Wasserstandes und der Strömungen in Randmeeren nebst Anwendungen, *Tellus,* **8** (1956), 287–300.
3. G. I. MARCHUK, About a numerical solution of the Poincare problem for ocean circulation, *Dokl. Akad. Nauk. SSSR,* **185** (1969), 1041–1044.

4. B. A. KAGAN, Hydrodynamic models of tidal motions in the sea, L. Gidrometeoizdat (1968).
5. G. I. MARCHUK, B. A. KAGAN, AND R. E. TAMSALU, A numerical calculation of tidal motions in adjacent seas, *Izv. Akad. Nauk SSSR Fiz. Atmosfer i Okeana* **5** (1969), 694–703.
6. B. A. KAGAN, On the resistance law for the tidal flow., *Izv. Akad. Nauk SSSR Fiz. Atmosfer. i Okeana* **8** (1972), 533–542.
7. O. A. LADYŽENSKAJA, Mathematical aspects of the dynamics of viscous incompressible fluid, M. Nauka (1970).
8. E. N. DVORKIN, B. A. KAGAN AND G. P. KLESHYOVA, The calculation of the tide motions in Arctic Seas, *Izv. Akad. Nauk. SSSR Fiz. Atmosfer. i Okeana* **8** (1972), 298–306.
9. V. YA. RIVKIND, On an estimate of the rate of conversion of homogeneous difference scheme for elliptic and parabolic equations with discontinuous coefficients, *in* "Boundary Value Problem and Integral Equations," (V. I. Smirnov, Ed.), Plenum, New York, 1968.
10. O. A. LADYŽENSKAJA AND V. YA. RIVKIND, On the alternating directions method for the calculation in cylindrical coordinates of the flow of a viscous incompressible fluid, *Izv. Akad. Nauk SSSR Ser. Mat.* **5** (1971), 259–269.